ROBUST CHANGE DETECTION IN URBAN AREA USING MULTI-TEMPORAL POLARIMETRIC UAVSAR DATA

Duk-jin Kim[1,2], Scott Hensley[1], and Sang-Ho Yun[1]

1. Jet Propulsion Laboratory, California Institute of Technology, USA
2. School of Earth and Environmental Sciences, Seoul National University, Korea

ABSTRACT

SAR change detection is useful when emergency situations occurred and weather conditions are unfavourable. In this study, a change detection using multi-temporal polarimetric UAVSAR data was investigated in urban environment. The most robust polarimetric parameter was evaluated, and change detction techniques using maximum likelihood ratio and hyperbolic tanget function were applied to the selected parameters. The comparison results with Google Earth's historical images showed a quite good agreement. A fitting of hyperbolic tangent function to the multi-temporal polarimetric parameters much reduced the false alarm rate, and it also provide whether the building was constructed or destructed and when the the changes occurred.

Index Terms— Change detection, polarimetry, UAVSAR, urban, multi-temporal

1. INTRODUCTION

Timely and reliable change information in urban areas is essential to city administrators and authorities in charge for planning and building safety. Thus, many techniques for identifying these changes have been investigated and developed. Optical remote sensing images have been mostly used for the detection of changes such as new buildings, roads, and even trees in the urban environment. Changed and unchanged areas can be effectively discriminated by optical multispectral data. However, such data are affected by clouds and illumination conditions. Synthetic Aperture Radar (SAR) is active microwave coherent imaging radar, so it has all-weather and day-and-night imaging capability. Furthermore, multi-polarization and multi-temporal SAR imagery can be expected to play an important role in change monitoring due to their unique scattering characteristics and data availability in regular interval. The traditional change detections have been carried out by applying the difference or ratio of multi-acquisition, image transformation, and the post-classification comparison [1-3]. More recent change detections were based on expert systems, such as artificial neural networks, fuzzy sets, and object-oriented approaches, or employing a new parameterization of the algebraic space [4]. These change detection algorithms were generally worked well in most applications, but they still suffer from non-trivial false alarm rates in urban environment. The objective of this study is to reduce false alarm rates and develop a more robust and reliable change detection algorithm in urban environment utilizing multi-temporal and polarimetric SAR data.

2. DATASETS AND POLARIMETRIC PARAMETERS

2.1. Datasets

The data used in this study were acquired by the NASA/JPL UAVSAR (Uninhabited Aerial Vehicle Synthetic Aperture Radar), which is an L-band airborne, polarimetric, repeat-pass, interferometric radar system [5]. The test site is the city of Pasadena, California, USA. The imaged area is a typical urban environment, consisting of buildings, roads, parks, and cars. A total of 11 sequential acquisitions covers a time interval of six years from 2009 to 2014. The nominal flight headings and altitudes were almost identical for all flights (the offsets between flight tracks were less than 10 m), because all the acquisitions of UAVSAR were supposed to be used for repeat-pass interferometry. Thus, the local incidence angles at fixed ground range positions can be considered almost the same in polarimetric point of view. The operational UAVSAR data products are provided in cross products (HHHH, HVHV, VVVV, HHHV, HVHV, and HVVV), which can be imported in the covariance matrix representation. The cross products (.grd files) are given in geographic ground projection with pixel spacing of 5.556e-5 by 5.556e-5 degree (which corresponds to about 5.12 by 6.16 m at the latitude of 34 degree). The data are multi-looked by 3 pixels in range and 12 pixels in azimuth.

2.2. Pre-processing

Although all polarimetric UAVSAR data are provided in geographic coordinates (latitude and longitude), a perfect matching between all corresponding pixels is required for change detection. Thus, a recently acquired data was selected as a reference image, and the rest images were co-registered to the reference image. For this co-registration process, 64 tie-points were generated to be used for determining the coefficients of 4^{th}-order mapping polynomial between a target image and the reference image. Each tie-point was selected using intensity cross-correlation between patch images (512×512) seized from the target and reference images. The implementation of the cross-correlation was conducted in power spectrum based on the Wiener-Khinchin theorem. The mapping polynomial was derived from only HHHH cross-product. The same mapping polynomial was applied to the rest of UAVSAR cross-products (HVHV, VVVV, HHHV, HVHV, and HVVV). We also applied the complex sinc interpolation for the resampling processing.

2.3. Polarimetric parameters

From the co-registered covariance matrixes $[C_3]$, more than 100 polarimetric parameters were extracted using PolSARpro version 4.2. The extracted parameters include intensities, intensity differences, phase differences, ratios, eigen-value set parameters, engen-vector set parameters, and polarimetric decompositions such as Freeman, VanZyl, Yamaguch, and Krogager decompositions.

3. CHANGE DETECTION MODEL

We tested more than 100 polarimetric parameters to evaluate which parameters are the most effective and robust for change detection in urban environment. The evaluation was conducted by calculating the separation of mean difference between the changed area and unchanged area with respect to the standard deviation in the unchanged area. The equation for the separation test can be expressed as follow:

$$\frac{|\overline{\Delta x_c} - \overline{\Delta x_u}|}{\sigma_u} \quad (1)$$

where, Δx represents the difference of polarimetric parameters between two acquisition times. The subscripts of c and u represent the changed and unchanged area, respectively. σ is the standard deviation of the difference. Fig. 1 shows results of the calculation for two regions. Both regions include the destroyed buildings for future rebuilding, but the buildings of first region are aligned in flight direction while the buildings of second region are obliquely aligned to the flight direction. The polarimetric parameters showing a good separability (greater than 1.5) were indicated in red (region 1) and green lines (region 2), respectively. It was found that the polarimeric parameters relevant to Shannon Entropy were most suited for change detection than any other polarimetric parameters. Double bounce component of polarimetric decompositions appears to work well for the buildings that are rightly facing to the radar look direction, but the rotated buildings were not detected using the double bounce parameters. The Shannon Entropy was not affected by the rotation of buildings, which is not surprising because Shannon Entropy is mostly determined by Eigen-values and they are all roll-invariant parameters as explained below.

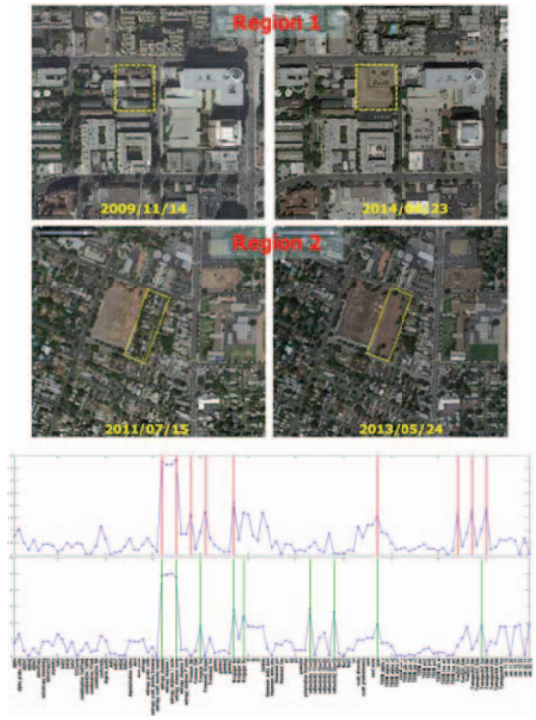

Fig. 1. Evaluation of separation between changed and unchanged areas for more than 100 polarimetric parameters.

In general, the Shannon Entropy (SE) can be calculated by

$$SE = 3\log\left(\frac{\pi e Tr(C_3)}{3}\right) + \log\left(27\frac{|C_3|}{Tr(C_3)^3}\right) \quad (2)$$

and the SE can be further developed as follow:

$$SE = \log\left(\frac{\pi^3 e^3 Tr(C_3)^3}{27} \cdot 27\frac{|C_3|}{Tr(C_3)^3}\right) \quad (3)$$

$$= \log(\pi^3 e^3 |C_3|) \quad (4)$$

As seen in this equation, the SE is proportional to the determinant of covariance matrix, which in turn, the multiplication of Eigen-values:

$$|C_3| = \prod_i \lambda_i\ , \quad \lambda_i = eigen(C_3) \quad (5)$$

Assuming that there are N time-series repeat-pass polarimetric SAR data, as the UAVSAR does, a multi-temporal polarimetric target vector is constructed by gathering the target vectors obtained at different times, t_i, $i = 1, 2, \ldots, N$.

$$\Omega_{MT} = [\Omega_{t_1} \quad \Omega_{t_2} \quad \cdots \quad \Omega_{t_N}]^T \quad (6)$$

where, $\Omega_{t_i} = [S_{hh}(t_i) \quad \sqrt{2}S_{hv}(t_i) \quad S_{vv}(t_i)]^T$ and T represents the transpose. Thus, the multi-temporal polarimetric covariance matrix is as follows

$$C_{MT-pol} = \langle \Omega_{MT} \Omega_{MT}^{+} \rangle = \begin{bmatrix} C_{11} & C_{12} & \cdots & C_{1N} \\ C_{21} & C_{22} & \cdots & C_{21} \\ \vdots & \vdots & \ddots & \vdots \\ C_{N1} & C_{N2} & \cdots & C_{NN} \end{bmatrix} \quad (7)$$

where, $C_{ii} = \langle \Omega_{t_i} \Omega_{t_i}^{+} \rangle$ and + represents conjugate.

On the other hand, multi-temporal change detection is usually conducted by assessing the variances of signals obtained in different time. Diagonal elements of Eq. (7) are the change of the stationary characteristic (i.e., the fluctuations of the variance of the signal). If the target's signal obtained by multi-temporal polarimetric SAR is stable (unchanged), then

$$\boldsymbol{H_0}:\ \boldsymbol{C_{11}} = \boldsymbol{C_{22}} = \cdots = \boldsymbol{C_{NN}} \tag{8}$$

The degree of changes (instability) can be measured using a maximum-likelihood ratio (Λ) [6]:

$$\boldsymbol{\Lambda} = \frac{\boldsymbol{max_{\Sigma}L(\Sigma,\cdots,\Sigma)}}{\boldsymbol{max_{\Sigma_{ii}}L(\Sigma_{11},\cdots,\Sigma_{NN})}} \tag{9}$$

For the polarimetric SAR data case, the signal sample variance is a (3×3) polarimetric coherency [T_3] or covariance matrix [C_3], thus the maximum-likelihood ratio of multi-temporal polarimetric SAR data is given by

$$\boldsymbol{\Lambda} = \frac{\prod_{i=1}^{N}|\boldsymbol{C_{ii}}|^{\boldsymbol{n_i}}}{|\boldsymbol{C_t}|^{\boldsymbol{n_t}}} \tag{10}$$

where, $\boldsymbol{C_t} = \frac{1}{n_t}\sum_{i=1}^{N}\boldsymbol{n_i C_{ii}}$ and $\boldsymbol{n_t} = \sum_{i=1}^{N}\boldsymbol{n_i}$. In Eq. (10), $|\ \ |$ represents the determinant of the matrix (which is similar quantity of Shannon Entropy as shown in Eqs. 2-4), and n_i represents the number of looks used in the estimation of the covariance matrices (ex., $n_i = 3 \times 12$ for UAVSAR GRD product).

This technique has already been adopted for time-frequency analysis using a single full-polarization SAR data [7, 8]. In this study, the technique was modified to apply for multi-temporal and dual- or full-polarization SAR data. Because full-polarization SAR data are not always available, in particular for space-borne SAR systems, the change detection with dual-polarization SAR data should be evaluated.

4. APPLICATION RESULTS

The maximum likelihood ratio using polarimetric covariance matrices was applied to multi-temporal UAVSAR data acquired from 2009 to 2014 in Pasadena (11 acquisitions) (Fig. 2). This technique is generally working well for detecting the constructed and destroyed buildings in urban environment (Fig. 3). However, it also detects some parking lots as changed places due to mobile cars (Fig. 3b). Another weakness of this technique is that it is difficult to know when the changes occurred.

In order to make more robust change detection (to rule out seasonal changes or mobile cars) and to know the time of change occurred, we employed a hyperbolic tangent function to fit into the temporal variation of polarimetric parameter (the determinant of covariance matrix) as below:

$$\widehat{|\boldsymbol{C}|}_{\boldsymbol{t_i}} = \boldsymbol{a} * \boldsymbol{tanh(t_i - b) + c} \tag{11}$$

where, the coefficients of *a*, *b*, and *c* are to be estimated using least-square method. The changed pixels were detected when |*a*| is greater than σ and *r*-square value is greater than 0.5 (Fig. 4). The sign of *a* can be used to indicate whether the building was constructed or destroyed, and *b* determines when the change occurred. The right image of Fig. 4 represents the detected pixels overlay in Google Earth (red and blue colors represent destroyed and constructed buildings, respectively). Because of the availability of multi-temporal UAVSAR data, the date of building construction/completion can also be constrained using the estimated coefficient of *b* (Fig. 5).

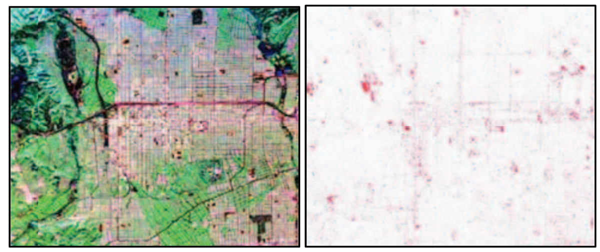

(a) (b)

Fig. 2. Change detection results in Pasadena city using multi-temporal and polarimetric UAVSAR data. (a) Study site represented by Freeman-Durden decomposition (red: double bounce, green: volume scattering, and blue: odd bounce), (b) detected changes using maximum-likelihood ratio (represented in red pots)

(a)

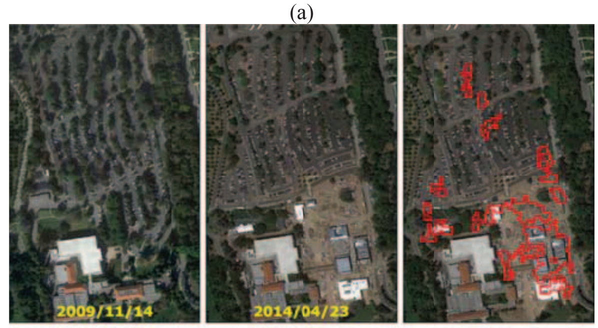

(b)

Fig. 3. Validation of change detection results using Google Earth's historical images. (a) Constructed buildings and (b) destroyed buildings.

Because full-polarimetric SAR data are not always availabe, we tested the change detection accuracy using dual-polarization SAR data. tests were conducted with the same multi-temporal UAVSAR data, but with the use of [C_2] instead of [C_3] (Fig. 6). The [C_2] matrix was constructed for the cases of HH & HV polarizations and HH & VV-polarizations. We also tested the similar change detection accuracy depending on the number of available multi-temporal datasets. The evaluations were carried out by comparing with the reference (the change detection reuslt of using full-polarimetric and whole 11 multi-temporal datasets) using the euqation below

$$y = \frac{\#of\ incorrectly\ detected\ pixels}{\#of\ correctly\ detected\ pixels} \tag{12}$$

The comparison results showed that the number of multi-temporal dataset was more sensitive to the detection accuracy than the number of polarizations.

Fig. 4. Change detection results (overlaid on Google Earth image) after fitting a hyperbolic tangent function. The red and blue dots represent destroyed and constructed buidlings, respectively.

Fig. 5. Detection of building completion dates using the coefficient of Eq. 11. The comparison with the housing information provided by a real estate website (zillow.com) showed a reasonable agreement.

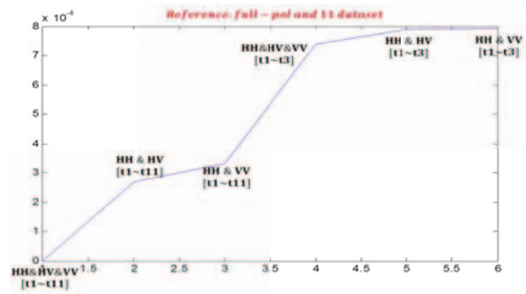

Fig. 6. Dependency of change detection accuracy on the numbers of polarization and multi-temporal datasets.

5. CONCLUSIONS

Robust change detection using multi-temporal polarimetric UAVSAR data was proposed and tested in this study. The Shannon Entropy and the determinant of polarimetric covariance matrix appear to be the most robust parameter in detecting changes in urban environment. A fitting of hyperbolic tangent function to the polarimetric parameters much reduced the false alarm detection rate, and further provided inforamtions about the construction/destruction of buildings and the date of change occurred. Dual-polarizations with a proper number of multi-temporal SAR datasets could be used for robust chage detection.

6. REFERENCES

[1] W. Dierking and H. Skriver, "Change detection for thematic mapping by means of airborne multitemporal polarimetric SAR imagery," *IEEE Transactions on Geoscience and Remote Sensing*, Vol. 40, No. 3, pp. 618-636, 2002.

[2] G. Moser and S.B. Serpico, "Unsupervised change detection from multichannel SAR data by markovian data fusion," *IEEE Transactions on Geoscience and Remote Sensing*, Vol. 47, No. 7, pp. 2114-2128, 2009

[3] Y. Bazi, L. Bruzzone, and F. Melgani, "An unsupervised approach based on the generalized gaussian model to automatic change detection in multitemporal SAR images," *IEEE Transactions on Geoscience and Remote Sensing*, Vol. 43, No. 4, pp. 874-887, 2005.

[4] A. Marino, S.R. Cloude, and J.M. Lopez-Sanchez, "A new polarimetric change detector in radar imagery," *IEEE Transactions on Geoscience and Remote Sensing*, Vol. 51, No. 5, pp. 2986-3000, 2013.

[5] S. Hensley, K. Wheeler, G. Sadowy, C. Jones, …, "The UAVSAR instrument: Description and first results,", *IEEE Radar Conference (RADAR'08)*, Rome, Italy, pp. 1-6, 2008.

[6] A.M. Mood, and F.A. Graybill, *Introduction to the Theory of Statistics, 2nd edition*, McGraw-Hill, 1963.

[7] L. Ferro-Famil, and E. Pottier, "Urban area remote sensing from L-band PolSAR data using Time-Frequency techniques," *Urban Remote Sensing Joint Event 2007*, France, pp. 1-6, 2007

[8] L. Ferro-Famil, A. Reigber, E. Pottier, and W.M. Boerner, "Scene characterization using subaperture polarimetric SAR data," *IEEE Transactions on Geoscience and Remote Sensing*, Vol. 41, No. 10, pp. 2264-2276, 2003.